New limit of the *G*-parity irregular weak nucleon current detected in β decays of spin aligned ^{12}B and ^{12}N

K. Minamisono, K. Matsuta, T. Minamisono, T. Yamaguchi, T. Sumikama, T. Nagatomo, M. Ogura, T. Iwakoshi, M. Fukuda, and M. Mihara
Department of Physics, Osaka University, 1-1 Machikaneyama, Toyonaka, Osaka 560-0043, Japan

K. Koshigiri
Department of Physics, Osaka Kyoiku University, 4-698-1 Asahigaoka, Kashiwara, Osaka 582-8582, Japan

M. Morita
Department of Physics, Josai International University, 1 Gumyo, Togane, Chiba 283-8555, Japan
(Received 19 June 2001; published 3 December 2001)

The *G*-parity irregular induced tensor form factor in the weak nucleon axial vector current has been precisely determined by measuring the alignment correlation terms in the β-ray angular distributions of the purely spin aligned mirror pair ^{12}B($I^\pi=1^+$, $T_{1/2}=20.2$ ms) and ^{12}N($I^\pi=1^+$, $T_{1/2}=11.0$ ms) in order to place a new limit on the applicability of the *G*-parity conservation law. The coefficient of the induced tensor term was determined to be $2Mf_T/f_A=-0.21\pm0.09$ (stat.) ±0.07 (syst.)±0.05 (theory) at a 90% confidence level. The previously obtained data in the year 1996 was reanalyzed to be added to the present result. The combined result is $2Mf_T/f_A=-0.15\pm0.12\pm0.05$ (theory) at a 90% confidence level. The obtained induced tensor coefficient is vanishingly small and is consistent with the theoretical prediction based on QCD in the framework of which the induced tensor form factor is proportional to the mass difference between up and down quarks. Also we set constraints on the Kubodera-Delorme-Rho parameters from the present result together with the results of correlation-type experiments in the mass $A=8$ and 20 systems as $\zeta=-(0.12\pm0.14)\times10^{-3}$ MeV^{-1} and $\lambda=+(0.30\pm0.88)\times10^{-3}$ in the 1σ level.

DOI: 10.1103/PhysRevC.65.015501 PACS number(s): 24.80.+y, 12.15.−y, 24.85.+p, 23.40.Bw

I. INTRODUCTION

In parity violating weak processes, *G*-parity symmetry is another important symmetry to be tested in order to clarify the validity of the symmetry between β decays of mirror pairs, namely, the proton and the neutron decays or more fundamentally between up and down quarks. Correctly subtracting the charge asymmetry between mirror pairs, the *G* symmetry may be broken because of the mass difference between mirror pairs or more fundamentally between up and down quarks. In this sense, the *G*-parity irregular term can be one of the keys to know how close we can get to the fundamental level of the nucleon β decay of zero momentum transfer as a direct decay of the quarks. We know well that the process of the nucleon or the nuclear β decay is the result of the quark decay, that is, $d\rightarrow u+e^-+\overline{\nu}$, inside the nucleon or the nucleus but the intrinsic process, the decay of a bare quark, cannot be detected directly. We may expect however that the emitted electron in β decay would carry information about the intrinsic process since the electron is a product of the direct decay of the quark. In extraction of this information, however, we need complete knowledge about the structure of the nucleus or the nucleon. One of the examples of the manifestation of the quarks inside the nucleon is the anomalous magnetic moment of the nucleon, which is well explained by the simple quark model. Also the mass difference between a neutron and a proton is shown to be caused by the difference in quarks making up the neutron (dud) and the proton (uud). Subtracting the effect of the charge of the proton, the difference of the mass becomes $M_n-M_p=2.05$ MeV, which is well reproduced by a calculation based on QCD [1].

The search for the *G*-parity irregular current in nuclear β decay has been continued since the classification under *G* transformation was introduced by Weinberg [2]. Recent development and the history of the search for the *G*-parity irregular term is well described in the article [3] by Wilkinson and the status of these investigations in the mid 1980s is described in a review article [4]. A great deal of work has been carried out especially in determining $ft_{1/2}$ value asymmetries in several pairs of mirror Gamow-Teller transitions [5]. As well, many correlation-type experiments have been carried out such as β-I correlation (β-ray angular distribution relative to the nuclear orientation) [6,7], β-α [8], and β-γ [9] angular correlations, particularly in the mass 8, 12, and 20 systems. The existence of the *G*-parity irregular current was not found within the relatively large experimental error. Still though, previous works did not exclude a small but finite amount of *G*-parity violation resulting from the mass and charge differences between the mirror pairs or up and down quarks [10,11]. Here, it is noted that the *G*-parity violation resulting from the charge difference was predicted to be of the order of the fine structure constant.

Since 1980, in order to place a new constraint on the *G*-parity irregular current in nuclear weak decay, we have continued to measure the alignment correlation term in the mass $A=12$ system. We have improved the experimental technique and also carefully examined systematic errors af-

fecting our results and conclusions [12,13]. Parallel to our experimental progress, advances have been made in understanding the axial charge asymmetry in mirror β decays [14] as well as on the relevant refined nuclear structure and wave functions of leptons in the β-decay process [15,16]. The latest value of the G-parity violating term derived from the alignment correlation experiment in the mass $A=12$ system [13] is $2Mf_T/f_A=+0.22\pm0.05$ (stat.)±0.15 (syst.)±0.05 (theory) in the 1σ level. This result however, has a large systematic error due to the spurious asymmetry in β-ray counting. In the present study this large systematic error was avoided by a newly developed timing program used for the measurement of the alignment correlation terms.

II. NUCLEAR β DECAY

A. Interaction Hamiltonian

Weak nuclear processes are described with the well-known current-current-type V-A interaction [15] as $H_I=\sqrt{1/2}(V_\lambda+A_\lambda)[\bar{\psi}_e\gamma_\lambda(1+\gamma_5)\psi_\nu]+$H.c., where V_λ and A_λ are the vector and the axial vector currents, respectively. Due to the strong interaction in the nucleus, Lorenz invariance allows for several other currents. As a result, the most general forms of the vector and the axial vector currents made up of the Dirac matrices γ_λ as well as the four-momentum transfer k_λ are given by

$$V_\lambda=\bar{\psi}_p(f_V\gamma_\lambda+f_W\sigma_{\lambda\rho}k_\rho+if_Sk_\lambda)\psi_n, \tag{1}$$

$$A_\lambda=\bar{\psi}_p\gamma_5(f_A\gamma_\lambda+f_T\sigma_{\lambda\rho}k_\rho+if_Pk_\lambda)\psi_n \tag{2}$$

with $\sigma_{\lambda\rho}=[\gamma_\lambda,\gamma_\rho]/2i$ and $k_\lambda=k_p-k_n$. Along with the main vector f_V and the main axial vector f_A currents, four other currents are included in the representation. They are the weak magnetism f_W, the induced scalar f_S, the induced tensor f_T, and the induced pseudoscalar f_P currents. The form factors are real if time-reversal invariance holds and generally they are the functions of k^2. The structure of the weak nucleon currents is characterized by the magnitudes of those six form factors in the vector and the axial vector currents and is well described in Ref. [17].

B. β-ray angular distribution from oriented nuclei

A theory of nuclear β decay was formulated by Morita *et al.* [15] in which higher-order corrections such as the Coulomb correction for the finite size of the nucleus and higher partial waves of the lepton wave function were properly taken into account. For the present experiment it is necessary to employ a formalism with higher-order corrections since we are concerned with the small recoil terms in the β decay. The β-ray angular distribution for the mass $A=12$ of ^{12}B and ^{12}N decaying into the ground state in ^{12}C, that is, (I^π, T, T_z: 1^+, 1, ∓1)$\rightarrow$(0^+, 0, 0) from oriented nucleus is given by

$$\frac{dW}{dEd\Omega}\propto pE(E_0-E)^2B_0(E)\left[1+P\frac{B_1(E)}{B_0(E)}P_1(\cos\theta)+A\frac{B_2(E)}{B_0(E)}P_2(\cos\theta)\right], \tag{3}$$

where $E(E_0)$ is the β-ray energy (end-point energy), θ is the angle between the polarization direction and the direction of the emitted β ray, p is the electron momentum, P_i are the Legendre polynomials, B_1/B_0 is the polarization correlation term, and B_2/B_0 is the alignment correlation term. These P and A are the degree of the nuclear spin polarization and the nuclear spin alignment, respectively, which are defined as $P=a_{+1}-a_{-1}$, $A=1-3a_0$ with $a_{+1}+a_0+a_{-1}=1$ for nuclear spin $I=1$, where a_i are the magnetic substate populations. Neglecting higher-order terms in the impulse approximation the alignment correlation term is simply described as

$$\frac{1}{E}\frac{B_2(E)}{B_0(E)}=\frac{2}{3}\left\{\pm\left(a-\frac{f_T}{f_A}\right)-\frac{y_\mp}{2M}\right\}, \tag{4}$$

where M is the nucleon mass and the subscript $\mp$ refers to electron or positron decays. The first term a in Eq. (4) is due to the weak magnetism and is given by the strong form of the conserved vector current (CVC) theory. The third term is the ratio of the timelike component in the main axial vector current, also called the axial charge and the main axial vector current $y=-2M\int i\gamma_5\boldsymbol{r}/\int\boldsymbol{\sigma}$. Thus, the correlation coefficient contains the weak magnetism term, the coefficient of the induced tensor term, and the axial charge.

C. G parity

G parity is the parity operation in charge space. The G transformation is defined by the product of the charge conjugation C and the charge symmetry operation $U=\exp(i\pi T_y)$, which is the rotation about the y axis by 180° in the charge space, as $G=C\exp(i\pi T_y)$. For instance, under the G transformation a neutron β^- decay current is transformed into a proton β^+ decay current. For the present nuclei, U relates the e^- decay of ^{12}B to the e^+ decay of ^{12}N whereas C relates the e^+ decay of ^{12}N to the e^- decay of $^{12}\overline{\text{N}}$. By CPT conservation, this is equivalent to the e^+ decay of ^{12}N. Each term of the hadronic weak current, $J_\lambda=V_\lambda+A_\lambda$, in Eqs. (1) and (2) is classified in terms of its behavior, $\Delta J_\lambda=\pm G\Delta J_\lambda G^{-1}$. G parities for those six terms are given by $G=+1$ for f_V, f_W, and f_T terms and $G=-1$ for f_A, f_P, and f_S terms. In the usual sign convention the leading term in the vector current transforms without change of sign under the G-parity operation and the leading term in the axial current changes sign. For instance, in the axial transition if the G parity of an exchange meson changes sign as that meson makes its contribution to the overall nuclear β decay, by itself β decaying between two nucleons, its contribution is G-parity regular and if it does not change sign its contribution is G-parity irregular. That is, those currents that are transformed as $GV_\lambda G^{-1}=+V_\lambda$ for vector current and $GA_\lambda G^{-1}=-A_\lambda$ for axial vector current are G-parity regular

and those transformed oppositely are *G*-parity irregular currents. If each current of Eqs. (1) and (2) has a definite *G* parity, the f_S and f_T terms should vanish because they have different *G* parities from those of their leading terms. Adopting the CVC theory, $\partial V_\lambda = 0$, we have $f_S = 0$. We cannot, however, set a similar constraint for the axial vector current since the pion decay to a muon is strictly forbidden under the condition $\partial A_\lambda = 0$. Weinberg first introduced the classification of these currents in terms of *G* parity [2]. Consequently in the weak nucleon currents only the f_T term in the axial vector current breaks *G* parity. If f_S exists this term does not appear in the $1^+ \rightarrow 0^+$ transition [4]. From the difference of the alignment correlation terms given in Eq. (4) between ^{12}B and ^{12}N, f_T can be extracted as

$$\left[\frac{1}{E}\frac{B_2(E)}{B_0(E)}\right]_{^{12}\mathrm{B}} - \left[\frac{1}{E}\frac{B_2(E)}{B_0(E)}\right]_{^{12}\mathrm{N}} = \frac{4}{3}\left(a - \frac{f_T}{f_A} + \frac{\Delta y}{2M}\right), \quad (5)$$

where Δy is the possible asymmetry in the axial charge defined as $\Delta y = [y_+(^{12}\mathrm{N}) - y_-(^{12}\mathrm{B})]/2$. On the other hand, the sum gives the axial charge as

$$\left[\frac{1}{E}\frac{B_2(E)}{B_0(E)}\right]_{^{12}\mathrm{B}} + \left[\frac{1}{E}\frac{B_2(E)}{B_0(E)}\right]_{^{12}\mathrm{N}} = -\frac{2}{3}\frac{y}{M}, \quad (6)$$

where $y = [y_+(^{12}\mathrm{N}) + y_-(^{12}\mathrm{B})]/2$. The axial charge is one of the most important parameters for the study on the meson exchange current in nuclei and the nuclear medium effect on the nucleon inside the nucleus. A detailed discussion on the axial charge can be found elsewhere [18].

III. EXPERIMENT

The ^{12}B and ^{12}N nuclei were produced at the Osaka University 4.75-MV Van de Graaff accelerator. The reaction chamber and part of the experimental apparatus are shown in Fig. 1. All the components of the experimental equipment other than counter telescopes and the electromagnet were contained in a steel vacuum chamber (not shown in the figure). Part of the chamber was made of plastic to reduce scattered β rays. The energy of the scattered electrons is very much reduced ($\sim$4 MeV) by the plastic before reaching the β-ray counters even if electrons are scattered by the steel wall. The experimental procedure consisted of four steps. These steps are summarized in the following Secs. III A, Production of the polarized nuclei; III B, Recoil implantation into the Mg catcher; III C and III D, Spin manipulation from polarization to alignment; III E, β-ray detection of the aligned nuclei.

A. Production of ^{12}B and ^{12}N

The ^{12}B(^{12}N) nuclei were produced through the nuclear reaction ^{11}B$(d,p)^{12}$B (^{10}B$(^3$He$,n)^{12}$N). A 1.5-MeV deuteron (3.0-MeV ^{3}He) beam provided by the 4.75-MV Van de Graaff accelerator at Osaka University was used to bombard a ^{11}B(98.0%; ^{10}B 2.0%) [^{10}B(90.4%; ^{11}B 9.6%) or ^{10}B(99.8%; ^{11}B 0.2%)] enriched reaction target (300 μg/cm^2) evaporated on a 0.15-mm-thick Mo backing ribbon

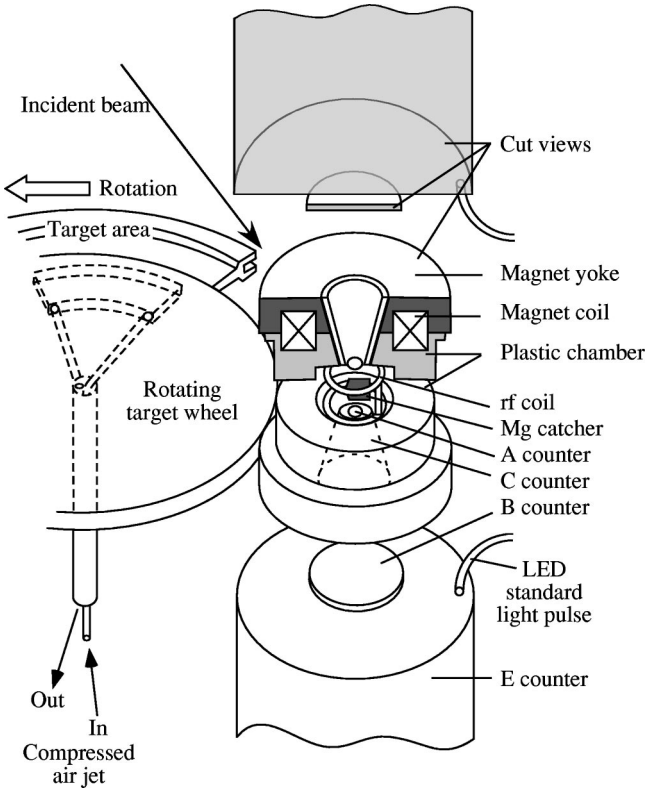

FIG. 1. Main part of the reaction and NMR chamber. The vacuum chamber is not shown in the figure. The part of the chamber close to the β-ray path to the counter system is made of plastic to reduce the scattered β rays. The target ribbon is attached to the rotating target system (target area), which rotates at a period of 75 ms. ^{12}B(^{12}N) produced through the nuclear reaction is implanted into Mg catcher and the β rays from the stopped nuclei are detected by the counter telescopes placed above and below the catcher.

(430 mm $\times$3.2 mm) attached to a rotating target holder with the grazing angle of 10° relative to the incident beam direction. The target, withstanding currents up to 30 μA, was cooled from inside the holder by a compressed air jet. A typical counting rate of β rays from stopped ^{12}B (^{12}N) in the Mg catcher detected by two sets of counter telescopes was 4 kcps (200 cps) at a beam intensity of 15 μA (30 μA). The target wheel rotated at a frequency of 75 ms. The Mo target ribbon was attached to one-third of the circumference of the target wheel as illustrated in Fig. 1. The pulsed incident beam was synchronized to the rotation of the target wheel so that we had the beam on target for 25 ms. During the beam-off time (50 ms), the target wheel was hidden in a radiation shield to avoid background radiation from the target, and during this time the β-ray counting and the spin manipulation were performed.

B. Recoil implantation

The produced ^{12}B (^{12}N) were ejected at a recoil angle 40°–75° (20°–55°), which was chosen by the target groove and the effective area of the catcher so that maximum polarization was obtained. The nuclei were then implanted into a recoil catcher of Mg single crystal (hcp) placed under an

external magnetic field of $H_0=600$ Oe applied parallel to the direction of the polarization. The typical size of the catcher was 15 mm $\times$20 mm in area and 500 μm in thickness. The maximum recoil energy of ^{12}B (^{12}N) was 0.44 MeV (1.5 MeV), and the maximum implantation depth in the catcher was 1.5 μm (2.7 μm). The energy spread resulting from the nuclear reaction and the target thickness, resulted in an implantation depth in the catcher distributed almost uniformly from the surface to the maximum depth. The polarization created through the nuclear reaction was about 10% (20%) and a small alignment of 2% (3%) was also produced. The degree of polarization produced was measured with the β-NMR (nuclear magnetic resonance) technique by detecting the asymmetric β-ray distribution relative to the polarization direction with a set of plastic scintillation counter telescopes placed above (up) and below (down) the catcher relative to the direction of the polarization axis.

C. Spin manipulation

1. Principle of the spin manipulation

The polarization resulting from the nuclear reaction was artificially converted into the alignment with, ideally, no residual polarization. By the use of spin manipulation, we were able not only to produce a large alignment compared with the small initial alignment produced through the nuclear reaction technique, but we were also able to create both positive and negative alignments. In this technique we use NMR with a magnetic interaction between the magnetic moment μ of ^{12}B(^{12}N) and an external magnetic field H_0 superposed on the electric interaction between a quadrupole moment Q of ^{12}B(^{12}N) and the electric field gradient q in the Mg single crystal. The crystal c axis of the Mg catcher was placed parallel to H_0. The interaction Hamiltonian is written as $H_I=H_M+H_E$, where

$$H_M=-\mu H_0,$$

$$H_E=\frac{eqQ}{4I(2I-1)}\left\{3I_Z^2-I(I+1)+\frac{\eta}{2}(I_+^2+I_-^2)\right\}. \quad (7)$$

Here, I is the nuclear spin of the implanted nucleus, eqQ/h is the quadrupole coupling constant, and I_+ (I_-) is the raising (lowering) operator of the magnetic substate m. For ^{12}B and ^{12}N in the Mg crystal, the electric field gradient is symmetric around the crystal c axis due to the symmetry of the crystal so that the asymmetry parameter η of the electric field gradient becomes zero $\eta=(V_{XX}-V_{YY})/V_{ZZ}=0$. Here the electric field gradient is defined by the principal components of $V_{ii}=d^2V/dX_i dX_i$ as $|V_{XX}|\leq|V_{YY}|\leq|V_{ZZ}|$ and $V_{ZZ}=q$. In the first-order perturbation calculation, the energy levels E_m for the magnetic substates m are unequally split because of the quadrupole interaction

$$E_m=-h\nu_L m+\frac{h\nu_Q}{6}\left(\frac{3\cos^2\beta-1}{2}+\eta\sin^2\beta\cos 2\gamma\right)\times\{3m^2-I(I+1)\},$$

$$\nu_Q=\frac{3eqQ}{2I(2I-1)h}. \quad (8)$$

Here, ν_L is the Larmor frequency and β and γ are the polar angles between the principal axis of the electric field gradient and the external magnetic field. In the present experimental condition $\beta=0°$ and $\eta=0$, the energy splits between the magnetic substates $m=1\leftrightarrow 0$, denoted F_H as a corresponding resonance frequency, and between substates $m=0\leftrightarrow -1$, denoted F_L, are well separated so that a specific transition between selected substates can be induced. Here the resonance frequencies are given in a first-order perturbation calculation by $F_H=\nu_L-\nu_Q/2$ and $F_L=\nu_L+\nu_Q/2$. The quadrupole coupling constant in Mg is known [19] to be $eqQ/h=-(47.0\pm0.1)$ kHz for ^{12}B and $eqQ/h=-(59.3\pm1.7)$ kHz for ^{12}N. The alignment was created from the polarization by use of spin manipulation. For the spin manipulation, two types of rf applications were used. One is an adiabatic fast passage (AFP) field denoted by $\vec{F}_L$ and $\vec{F}_H$, which interchanges the populations of two specific magnetic substates. A typical AFP-field condition for ^{12}B and ^{12}N was $F_M=\pm15$ kHz, $t_{\rm rf}=1$ ms, and $H_1\sim10$ Oe, where F_M is the frequency modulation, $t_{\rm rf}$ is the rf-sweep time, and H_1 is the magnitude of rf, respectively. The other is a depolarization (D) field denoted by $\bar{F}_L$ and $\bar{F}_H$, which equalizes the populations of two specific magnetic substates. A typical D-field condition was $F_M=\pm10$ kHz, $t_{\rm rf}=2$ ms, and $H_1\sim5$ Oe. Applying a set of rf fields, the population in the unequally separated magnetic substates are equalized and/or interchanged so that the positive and the negative alignment are produced.

2. Timing program for the creation of alignment

The spin manipulation for the artificial creation of the alignment and β-ray detection were performed in accordance with the timing programs controlled by a microcomputer. There were two types of newly developed timing programs used in this experiment. One was a timing program named ''main sequence'' program for the creation of the positive and the negative alignment and the measurement of β-ray energy spectra from the aligned nuclei. The other was a timing program named ''test sequence'' program in which the efficiency of the spin manipulation was checked. Each program consisted of several production beam cycles synchronized with the rotating target.

a. Main sequence program. A set of main sequence programs processed four kinds of beam cycles, which are illustrated in Fig. 2. The $A_M^{\pm}$ and $A_M^{\mp}$ cycles for the production of the positive and negative alignment were the principal part of the experiment and measured the β-ray spectra from the aligned nuclei. In the $A_M^{\pm}$ cycle, by applying a depolarizing field $\bar{F}_H$ before counting portion I and sequentially applying

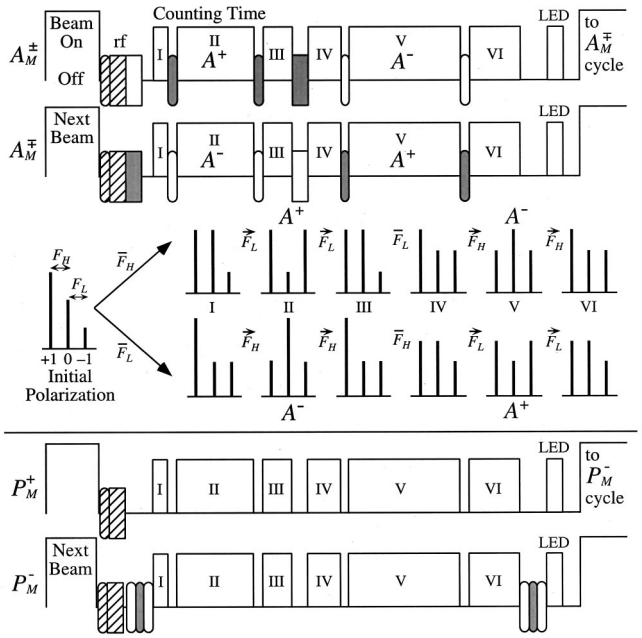

FIG. 2. New timing program (main sequence program) and magnetic substates populations. The main sequence program is illustrated in which positive and negative alignment are produced. The regions labeled from I to VI are the counting times. The squares and the ellipses between the counting times represent the rf for spin manipulation. The rf hatched with gray represents the production of positive alignment, white represents negative alignment, and hatched lines the destruction of the second component. The $A_M^{\pm}$ and $A_M^{\mp}$ cycles are shown in the upper part of the figure together with the change of the magnetic substates populations by the spin manipulation. After the spin manipulation by use of the NMR technique was completed following the end of the production time, β-ray counting was started. In the lower part, the P_M^+ and P_M^- cycles are shown from which g was determined. A set of main sequence program consistend of 20 pairs of $A_M^{\pm}$ and $A_M^{\mp}$ cycles, which were followed by 10 pairs of P_M^+ and P_M^- cycles. The sets were repeated until the preset counting statistics were obtained.

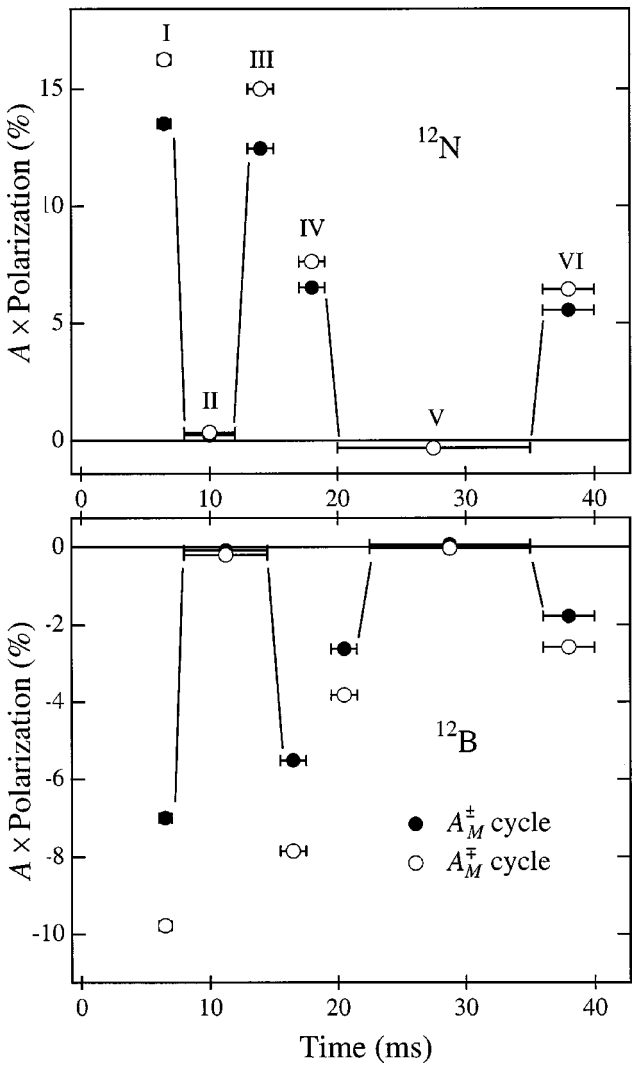

FIG. 3. Typical result of the spin manipulation in the main sequence program. The upper part of the figure is the result of ^{12}N and the lower part of ^{12}B. A in the ordinate is the asymmetry parameter (-1 for ^{12}B and $+1$ for ^{12}N). The full circles are for the polarization change in the $A_M^{\pm}$ cycle and the open circles, in the $A_M^{\mp}$ cycle. The lines in the figure schematically illustrate the change of the polarization by the spin manipulation. At time zero, the incident beam was chopped. The alignments were successfully created in portions II and V. The smaller polarization in $A_M^{\pm}$ cycle relative to that in the $A_M^{\mp}$ cycle is due to the initial alignment produced through the nuclear reaction.

an AFP field $\vec{F}_L$ before counting portion II, we obtained the positive alignment in portion II. To confirm the alignment in portion II, the alignment was converted back again into the polarization in portion III. Right after counting portion III, alignment with the opposite sign was produced in counting portion V. To start from the negative alignment in another beam cycle of $A_M^{\mp}$, we replaced the $\bar{F}_H$ and $\vec{F}_L$ rf set with the $\bar{F}_L$ and $\vec{F}_H$ rf set. The typical result of the polarization changes in $A_M^{\pm}$ and $A_M^{\mp}$ as a function of time are illustrated in Fig. 3. The alignments were successfully created in portions II and V. The other parts of the main sequence program were the P_M^+ and P_M^- cycles for the measurement of the geometrical center. These cycles were performed to determine the counting rate ratio g corresponding to zero polarization. As shown in Fig. 2 the time-dependent decay of the polarization produced through the nuclear reaction was measured in the P_M^+ cycle with no rf, while in the P_M^- cycle the time-dependent decay of the inverted polarization created by $\vec{F}_H$-$\vec{F}_L$-$\vec{F}_H$ rf was measured. A set of the main sequence program consisted of 20 pairs of $A_M^{\pm}$ and $A_M^{\mp}$ cycles, which were followed by 10 pairs of P_M^+ and P_M^- cycles. The set was repeated until a preset counting statistics were obtained. An ideal spin manipulation yields the alignment as $A_{\mathrm{II}}^{\pm}=(\pm 3P_0-A_0)/2$ and $A_{\mathrm{V}}^{\mp}=(\pm 3P_0-A_0)/4$, where P_0 is the initial polarization, A_0 is the initial alignment produced through the nuclear reaction, and $A_i^{\pm}$ is the alignment created in counting portion i. The difference of the positive and the negative alignment becomes 4.5 times larger than the initial polarization $\hat{A}=(A_{\mathrm{II}}^+-A_{\mathrm{II}}^-)+(A_{\mathrm{V}}^+-A_{\mathrm{V}}^-)=4.5P_0$, which reached actual values of 40% for ^{12}B and 85% for ^{12}N as

TABLE I. Result of the spin manipulation. As defined in Sec. III C 2, P is the initial polarization produced through the nuclear reaction, α is the efficiency of the spin inversion defined by the inverted $P'=\alpha P$, $\eta(F_L)$ [$\eta(F_H)$] is the efficiency for creation of the positive (negative) alignment, $\hat{A}=(A_{\rm II}^{+}-A_{\rm II}^{-})+(A_{\rm V}^{+}-A_{\rm V}^{-})$, is the effective alignment, $\Delta P=(P_{\rm II}^{+}-P_{\rm II}^{-})+(P_{\rm V}^{+}-P_{\rm V}^{-})$ is the residual polarization in alignment section, and $T_1(P)$ [$T_1(A)$] is the spin lattice relaxation time of the polarization (alignment).

	^{12}B	^{12}N
P (%)	11.25±0.01	20.12±0.06
α (%)	−94.8±0.04	−94.9±0.09
$\eta(F_L)$ (%)	98.13±0.08	99.1±0.3
$\eta(F_H)$ (%)	98.29±0.07	99.1±0.3
$\hat{A}$ (%)	39.99±0.06	84.2±0.4
ΔP (%)	−0.09±0.01	0.28±0.05
$T_1(P)$ (ms)	78.1±0.4	247±3
$T_1(A)$ (ms)	30.4±0.3	75±8

listed in Table I. This large effective alignment makes the experiment very efficient and reliable.

b. Test sequence program. Though an ideal spin manipullisted in Table I. This large effective alignment makes the ation yields the difference of the positive and the negative alignment to $\hat{A}=4.5P_0$, actually $\hat{A}$ varied from the ideal amount because of the imperfect efficiency of the spin manipulation. To determine the true alignment, the efficiency for the interchange of two specific populations of magnetic states ($a_i \leftrightarrow a_{i+1}$) had to be measured in a set of test sequence program. As shown in Fig. 4 five kinds of beam cycles were used for this determination. They were $A_T^{\pm}$ and $A_T^{\mp}$ cycles for the measurement of the degree of achievement of spin manipulation for the creation of the positive and the negative alignment, respectively. The procedure of the test sequence program was the same as that of the main sequence program except for the absence of counting portions II and V, where the β-ray energy spectrum from the aligned nuclei was measured. Right after the alignment was produced, the alignment was immediately converted back again to polarization. Thus, the deviation between the initial and the final polarization represents the achievement of the applied rf field and T_1. A typical result of the polarization change as a function of time in test sequence program is illustrated in Fig. 5, where part of the beam cycles are shown. In addition, P_T^{+}, P_T^{-}, and P_T^{++} cycles measured g and T_1 by detecting the time-dependent decay of the initial polarization. The test sequence program was performed for 1h (2 h) in every 5-h (10-h) run of the main sequence program in ^{12}B (^{12}N) experiment. The results of spin manipulation are summarized in Table I. In the table P is the initial polarization produced through the nuclear reaction, α is the efficiency of the spin inversion defined by the inverted $P'=\alpha P$, $\eta(F_L)$ [$\eta(F_H)$] is the efficiency for creation of the positive (negative) alignment, $\hat{A}=(A_{\rm II}^{+}-A_{\rm II}^{-})+(A_{\rm V}^{+}-A_{\rm V}^{-})$ is the effective alignment, $\Delta P=(P_{\rm II}^{+}-P_{\rm II}^{-})+(P_{\rm V}^{+}-P_{\rm V}^{-})$ is the residual polarization in the alignment portion, and $T_1(P)$ [$T_1(A)$] is the spin lattice relaxation time of the polarization (alignment).

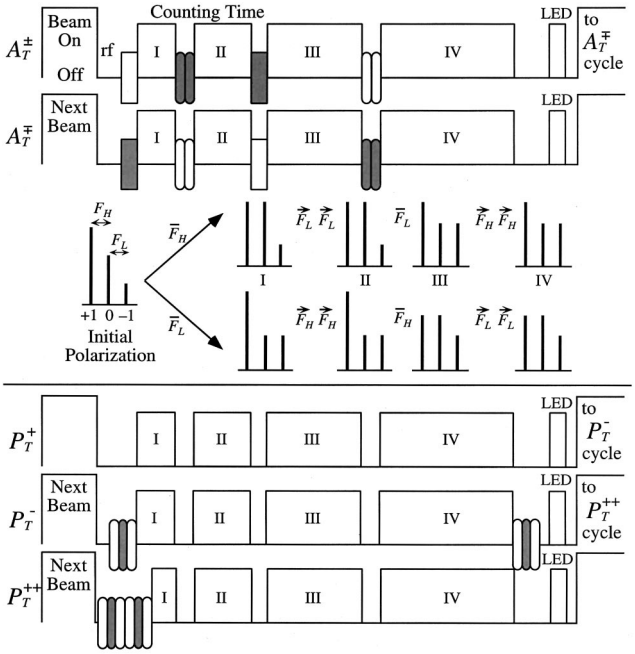

FIG. 4. New timing program (test sequence program) and magnetic substates populations. The test sequence program is illustrated in which the efficiency of the spin manipulation were measured. The regions labeled from I to IV are the counting times. The squares and the ellipses between the counting times represent the rf for spin manipulation. The rf hatched with gray represents the production of positive alignment and white represents negative alignment. The $A_T^{\pm}$ and $A_T^{\mp}$ cycles are shown in the upper part of the figure together with the change of the magnetic substates populations by the spin manipulation. In the lower part the P_T^{+}, P_T^{-}, and P_T^{++} cycles are shown from which the geometrical center g and the spin lattice relaxation time T_1 were determined. The test sequence program was performed for 1 h (2 h) in every 5-h (10-h) run of the main sequence program in ^{12}B (^{12}N) experiment.

D. Mg catcher

A catcher was cut out from a bulk Mg single crystal so that the c axis was in the plane of the catcher. For the cutting, a spark slicer was used to minimize the damage on the surface of the crystal. In the next step, the surface of the catcher was etched by 50 μm at room temperature with citric acid (5% concentration) to the thickness of about 500 μm, to remove damages and defects on the surface produced by the slicing process. After the etching, the residuals on the surface were quenched by deionized water and the water was blown off by a jet of dry N_2 gas. The x-ray diffraction pattern of the crystal was checked to confirm the orientation of the c axis and the structure near the surface. The Mg catcher was mounted on the tip of an Al holder of 0.5 mm thickness, which was attached on the coil holder along with an rf coil. The backing was cooled by water flow to prevent heating due to irradiation of the production target and from eddy currents created by the rf fields. During the experiment, the surface of the catcher slowly became contaminated by the sputtered target due to beam irradiation. This resulted in a decrease in the measured polarization. To remove the contamination and to recover the polarization, the surface of the

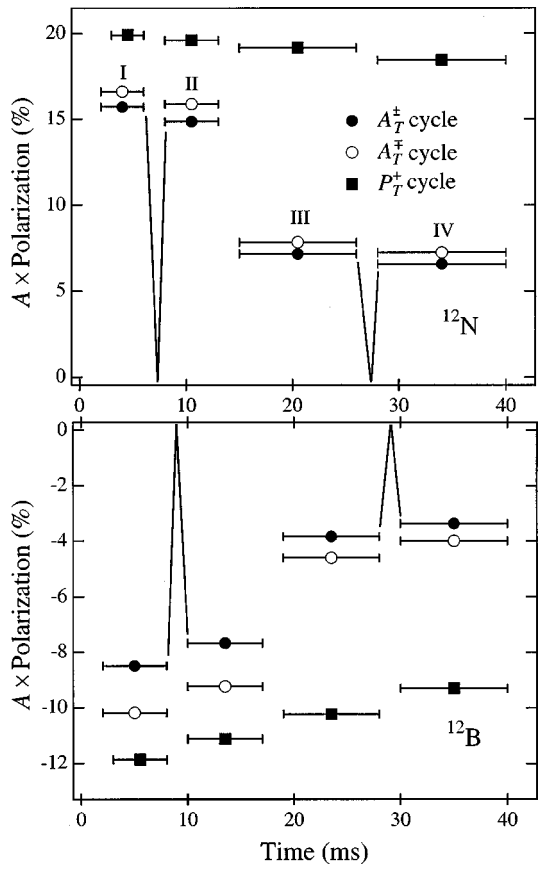

FIG. 5. Result of the spin manipulation in test sequence program. The upper part of the figure is for ^{12}N and the lower part for ^{12}B. *A* in the ordinate is the asymmetry parameter (-1 for ^{12}B and $+1$ for ^{12}N). The full circles are for the polarization change in the $A_T^{\pm}$ cycle and the open circles, in the $A_T^{\mp}$ cycle. The lines in the figure schematically illustrate the change of the polarization by the spin manipulation. An alignment was created between the counting portions I and II (III and IV) and immediately converted back to polarization. The difference of the polarization between portions I and II (III and IV) is due to the efficiency of the manipulation and to the T_1. The full squares are for the polarization change in the P_T^{+} cycle in which no rf was applied for the measurement of T_1.

Mg catcher was etched every 72 h. For reliable spin manipulation accurate knowledge of the quadrupole interaction is very important. Recently, we found a new minority location of ^{12}B and ^{12}N in Mg (second component) [19], which might affect the result of the spin manipulation and, in the worst case, would have about 15% of population relative to the population of the well-known majority location (main component). From detailed studies, it has been shown that (1) the second component is caused by micrograins introduced into the crystal during the growth process and/or of the cutting and treatment of the crystal, (2) the *c* axis of the micrograin is perpendicular to that of the bulk crystal, and (3) the absolute value of the electric field gradient for the second component is the same as that for the main component and perpendicular to the *c* axis of the bulk crystal. The coupling constant for the second component is $eqQ/h \sim -45$ kHz for ^{12}B and $eqQ/h \sim -60$ kHz for ^{12}N with *q* vertical to the *c* axis of the bulk crystal. The amount of the second component is strongly dependent on the way the surface of the Mg catcher is treated. Thus, in the present experiment a spark slicer was used for cutting out a catcher and its surface was etched. Every time a newly treated catcher was used, the amount of the second component was shown to be zero, $P=0$, within the experimental error by detecting the NMR signal from that component. To ensure the absence of the effects from the second component in the final result, we destroyed the polarization of the second component by applying a set of rf fields before each measurement of the energy spectra as illustrated in Fig. 2. Moreover, since the crystal *c* axis of Mg catcher was placed parallel to the external magnetic field, the two sets of resonance frequencies resulting from the main and the second component were well separated. Thus the spin manipulation for the main component was not affected by the second component at all.

E. β-ray energy spectrum

1. β-ray detectors

The β rays from aligned ^{12}B and ^{12}N in counting portions II and V were detected with a 150 mm$\phi\times$175 mm plastic scintillation counter named the *E* counter. The counter was large enough to measure the entire β-ray energy and was placed above (up) and below (down) the catcher relative to the polarization direction. The counter system telescope is shown in Fig. 1. The solid angle of each telescope (1.4×10^{-2} sr/4π) was defined by two sets of thin plastic scintillation counters named the *B* counter (55 mm$\phi\times$1 mm) placed right in front of the *E* counter and a counter named the *A* counter (12 mm$\phi\times$0.5 mm), which was placed close to the catcher. The cone shaped plastic scintillation veto counter named the *C* counter was used to reject unwanted β rays scattered by the return yokes of the air core β-NMR magnet. To prevent the photomultiplier tubes (PMTs) of the *E* counter from saturation due to the prompt radiation during production time, the high voltage fed to the first dynode of the PMTs was dropped during beam-on time so as not to amplify those photoelectrons. Using this method we were able to avoid unwanted effects in the β-ray counting time. Because of the long data acquisition time (several weeks), the stability of the energy counter system had to be very high for the accurate determination of the alignment correlation terms. In the experiment, a pulse-height-gain stabilizer was used in the amplifier system. A standard light pulse from an light-emitting diode (LED) pulser maintained at a constant temperature was used at the end of every beam cycle to ensure the stability of the *E* counter, as illustrated in Figs. 2 and 4. The stability of the counter system was monitored by the change in the center of gravity of the β-ray energy spectrum and the variation of the center of gravity was found to be within $(0\pm1)\%$ for both the ^{12}B and ^{12}N spectra. This stability was sufficient for the precise measurement of alignment correlation terms. The small time-dependent energy shift was properly taken into account as a systematic error as discussed later.

2. Trigger signal

Real events were selected by the trigger signal $A\cap B\cap\overline{C}\cap E$ in the coincidence unit. Furthermore, two sig-

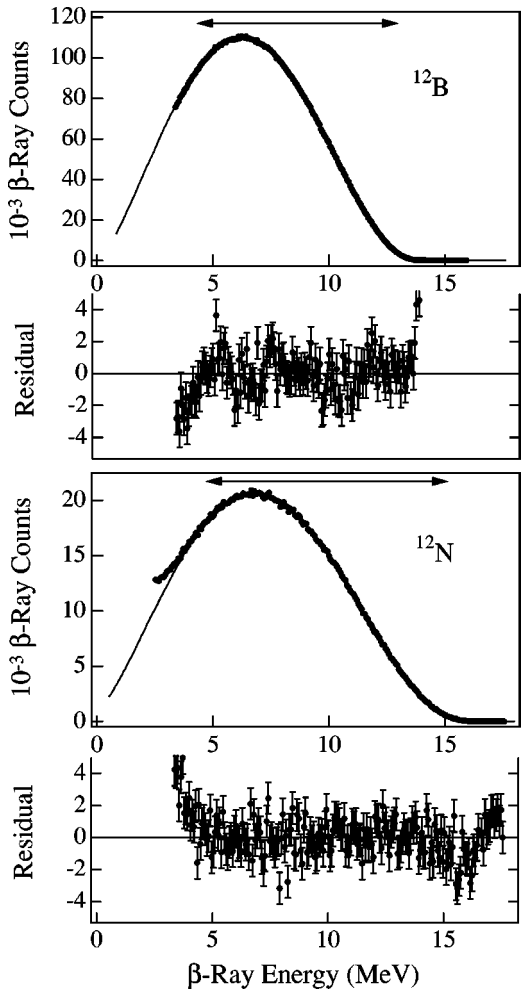

FIG. 6. β-ray energy spectrum of ^{12}B and ^{12}N. The upper part shows a typical energy spectrum of ^{12}B and the lower part of ^{12}N. The dots are the experimental data and the solid lines are the best fit of the simulated energy spectrum to the data. Together with the spectrum, the residuals $(N_{\rm exp}-N_{\rm fit})/N_{\rm exp}^{1/2}$ are plotted, where $N_{\rm exp}$ and $N_{\rm fit}$ are the experimental data and the fit result, respectively. The errors are from the experimental data. The fitting regions were 4.1–13.0 MeV for ^{12}B and 4.6–15.1 MeV for ^{12}N indicated by arrows. For this typical spectrum we had $\chi^2/\nu=1.29$ for ^{12}B and $\chi^2/\nu=1.00$ for ^{12}N.

nals arriving within the timing interval of 500 ns were rejected as pile-up events. The signals from these rejected events were consistent with back-scattered β rays or cosmic rays. The resultant events were further inhibited during the 10 μs busy time of the analog-to-digital converter (ADC). All the discriminators were inhibited during beam-on time and rf time.

3. Linear signal

To ensure as high a counting rate as possible the linear signals obtained from the dynode of the PMT (HAMAMATSU R1250) of an E counter had a relatively short decay constant of about 1 μs and were further shortened by the delay line clipping method to about 500 ns. After the clipping they were selected by the trigger signals mentioned above to reject all the unwanted events. The selected true events were digitized by the ADC after being amplified. The spectrum data were finally read out through a CAMAC crate controller. The linear signals that originated from the LED standard light pulser were led to the gain stabilizer loop. The gain shift of the system, detected by the change of pulse height of the LED light, was fed back to the amplifier so as to cancel the gain shift.

4. Counter response function

The β-ray energy spectrum from unoriented nuclei is given as

$$S(E)=pE(E_0-E)^2F(\pm Z,E)[1+R_0(E,E_0)], \qquad (9)$$

where $F(\pm Z,E)$ is the Fermi function and $R_0(E,\ E_0)$ is the radiative correction. The measured β-ray spectra, however, varied from the shape given by $S(E)$ because of the response of the β-ray counter. β rays in the plastic scintillation counter loose kinetic energy by electric excitation in the plastic and by the bremsstrahlung process. Since the energy deposition by the monochromatic β ray in the plastic has a low energy tail in the pulse height spectrum, because a part of the bremsstrahlung may escape from the surface of the counter without depositing its energy in the counter, and also has a high energy tail because of the positron annihilation, a simple minded theoretical response function does not reproduce the lower energy tail and the shape at the higher energy tail at all. Scattered β rays in the Mg catcher also contributed to the lower energy tail. Thus in the present analysis the character of the monochromatic β-ray energy deposition was studied based on Monte Carlo simulation of the electromagnetic cascade shower EGS4 [20]. The response function $R(x,E)$ of β ray with monochromatic energy E is dependent upon the energy deposit function $f(y,E)$, which was simulated using the EGS4 code taking into account the geometry of the counter system and the NMR chamber and the effects of annihilation gamma in flight and also the one or two photons escaped in scintillator were taken into account. The response function is given by the energy deposit function convoluted with the counter resolution

$$R(x,E)=\int f(y,E)\frac{1}{\sqrt{2\pi}\sigma}\exp\left[-\frac{(x-y)^2}{2\sigma^2}\right]dy. \qquad (10)$$

Here x is the observed energy, y is the energy deposit, and σ is the resolution of the counter, where σ is expected to have the form $\sigma_0\sqrt{E}$ and σ_0 is a constant. Thus, the observed energy spectrum $W(E)$ is given by the statistical shape $S(E)$ in Eq. (9) convoluted with the response function

$$W(E)=\int S(\mu)R(E,\mu)d\mu, \qquad (11)$$

where E is the observed energy and μ is the incident energy. The reliability of the simulation was checked by measuring monochromatic β^+ and β^- rays using a spectrometer. From the experimental check, we find a $(0\pm20)\%$ difference between the lower energy tail of the shape of the experimental

response function and that of simulated one, which was taken into account in evaluating a systematic error. The obtained simulated energy spectrum was used for the least χ^2 fitting to the measured energy spectra. A typical result of the fitting is shown in Fig. 6. The fitting parameters were the zero energy channel, the end-point channel, and the normalization of the amplitude. In this fit, the counter resolution $\sigma_0 = 0.12\ \mathrm{MeV}^{-1}$ for the up counter system and $\sigma_0 = 0.08\ \mathrm{MeV}^{-1}$ for the down counter system were used. These values were determined by fitting the simulated energy spectrum to another set of experimental data obtained for the determination of the resolution. We found excellent agreement between the simulated spectrum and the experimental data.

5. Energy scaling

The energy scale was determined by measuring the end-point energies of β-ray spectra from several β emitters produced through nuclear reactions. For the ^{12}B experiment, $^{12}\mathrm{B}(E_{\mathrm{end}} = 13.369\ \mathrm{MeV})$, $^{20}\mathrm{F}(E_{\mathrm{end}} = 5.390\ \mathrm{MeV})$, and $^{28}\mathrm{Al}(E_{\mathrm{end}} = 2.863\ \mathrm{MeV})$ were produced and measured. For the ^{12}N experiment, $^{12}\mathrm{N}(E_{\mathrm{end}} = 16.3161\ \mathrm{MeV})$, $^{30}\mathrm{P}(E_{\mathrm{end}} = 3.210\ \mathrm{MeV})$, and $^{15}\mathrm{O}(E_{\mathrm{end}} = 1.732\ \mathrm{MeV})$ were produced and measured. In the extraction of the end-point energy, the least χ^2 fitting of the simulated energy spectrum was performed in which the free parameters were the zero-point energy, the end-point energy, and the normalization factor.

IV. ANALYSIS

A. Principle of the extraction of B_2/B_0

The alignment correlation term can be extracted from the β-ray counting ratio of positively and negatively aligned nuclei for a given β-ray energy $\hat{E}_i = E_i \pm \Delta E$. In this analysis, E_i ranged from 5 MeV to 13 MeV in total energy for ^{12}B and from 5 MeV to 15 MeV in total energy for ^{12}N and $\Delta E = 0.5$ MeV. The double ratio of up or down counters in portions II and V in the main sequence program is defined by

$$R_{U\mathrm{or}D}(\hat{E}_i) = \left[\frac{T^{\pm} N^{+}_{\mathrm{II}}(\hat{E}_i)}{T^{\mp} N^{-}_{\mathrm{II}}(\hat{E}_i)} \frac{T^{\mp} N^{+}_{\mathrm{V}}(\hat{E}_i)}{T^{\pm} N^{-}_{\mathrm{V}}(\hat{E}_i)} \right]_{U\mathrm{or}D} = \left[\frac{B_0(\hat{E}_i) \pm P^{+}_{\mathrm{II}} B_1(\hat{E}_i) + A^{+}_{\mathrm{II}} B_2(\hat{E}_i)}{B_0(\hat{E}_i) \pm P^{-}_{\mathrm{II}} B_1(\hat{E}_i) + A^{-}_{\mathrm{II}} B_2(\hat{E}_i)} \frac{B_0(\hat{E}_i) \pm P^{+}_{\mathrm{V}} B_1(\hat{E}_i) + A^{+}_{\mathrm{V}} B_2(\hat{E}_i)}{B_0(\hat{E}_i) \pm P^{-}_{\mathrm{V}} B_1(\hat{E}_i) + A^{-}_{\mathrm{V}} B_2(\hat{E}_i)} \right]_{U\mathrm{or}D}, \tag{12}$$

where $T^{\pm}$ and $T^{\mp}$ are the possible time-dependent asymmetry in the β-ray counting in $A^{\pm}_M$ and $A^{\mp}_M$ cycles caused by the intensity fluctuation of the incident beam, $N^{\pm}_i$ are the β-ray counting from the positive $+$ and the negative $-$ alignments in counting portion i in the main sequence program, and the upper and lower signs are for up and down counters, respectively. Here it should be noted that in Eq. (12) the time-dependent asymmetry $T^{\pm}$ and $T^{\mp}$ are completely canceled out. Neglecting higher-order contributions from the alignment and the residual polarization, the alignment correlation term is ideally given by

$$\left[\frac{B_2(\hat{E}_i)}{B_0(\hat{E}_i)} \right]_{U\mathrm{or}D} \cong \frac{R_{U\mathrm{or}D}(\hat{E}_i) - 1 \mp \Delta P}{\hat{A}}, \tag{13}$$

where $\hat{A} = (A^{+}_{\mathrm{II}} - A^{-}_{\mathrm{II}}) + (A^{+}_{\mathrm{V}} - A^{-}_{\mathrm{V}})$ is the effective alignment and $\Delta P = (P^{+}_{\mathrm{II}} - P^{-}_{\mathrm{II}}) + (P^{+}_{\mathrm{V}} - P^{-}_{\mathrm{V}})$ is the residual polarization caused by the imperfect spin manipulation, which was negligibly small $|\Delta P/\hat{A}| \leqslant 0.35\%$ as shown in Table I. Moreover, summing the alignment correlation terms obtained from up and down counters, the small but finite effects of the residual polarization can be rejected as

$$\frac{B_2(\hat{E}_i)}{B_0(\hat{E}_i)} = \frac{1}{2} \left\{ \left[\frac{B_2(\hat{E}_i)}{B_0(\hat{E}_i)} \right]_U + \left[\frac{B_2(\hat{E}_i)}{B_0(\hat{E}_i)} \right]_D \right\} \cong \frac{1}{2\hat{A}} [R_U(\hat{E}_i) - 1 + R_D(\hat{E}_i) - 1]. \tag{14}$$

In the actual analysis the higher-order contributions from the alignment and the small residual polarization were properly taken into account by directly solving Eq. (12).

B. Weak magnetism

We shall extract the strength of the induced tensor current from the experimental data on the β-ray asymmetry. As is seen in Eq. (5), this is possible if the weak magnetism is given to a good precision. In the strong form of the CVC, the weak magnetism appears in the ratio of the nuclear matrix elements of the vector and the axial vector current,

$$a = -\frac{1}{2M} \frac{\int V}{\int A} = -\frac{1}{2M} \frac{f_V \left\{ (1 - 2M f_W/f_V) \int \boldsymbol{\sigma} + \int \boldsymbol{l} \right\}}{f_A \int \boldsymbol{\sigma}} = -\frac{1}{2M} \frac{f_V}{f_A} \left(1 + \mu_p - \mu_n + \frac{\int \boldsymbol{l}}{\int \boldsymbol{\sigma}} \right), \tag{15}$$

where μ_p and μ_n are the anomalous magnetic moments of

the free nucleon with $\mu = 1 + \mu_p - \mu_n = 4.706$. In this expression we have suppressed exchange currents terms for simplicity.

The presence of the weak magnetism is direct proof of the strong form of CVC, namely, the universality of the magnetic form factors between the isovector component of the electromagnetic and the weak interactions. As a result many experiments to detect the weak magnetism have been performed. In these experiments, the spectral shape in the β-ray energy spectrum is slightly affected by the weak magnetism and is given by $dW_{\mp}(E)/dE \propto pE(E_0 - E)^2(1 \pm 8aE/3)$. Although several measurements of the spectral shape factor have been performed [21], we did not use those experimental results in determining the value of the weak magnetism. The precision of the results is not high due to the unavoidable β-ray scattering problem and the lack of the knowledge of the detectors response to monochromatic β rays, although all the data are consistent with the CVC prediction.

The best quantity to determine the weak magnetism is the transition strength of the $M1$-γ ray decaying from the 15.11-MeV excited state in ^{12}C to its ground state. The 15.11-MeV state forms an isospin triad together with the ground states of ^{12}B and ^{12}N. We use the transition rates of the mass $A = 12$ system in β and γ decays to evaluate the magnitude of the weak magnetism and we modify the formula (15) slightly as below,

$$2a = a_- + a_+ \tag{16}$$

with

$$\begin{aligned} a_{\mp} &= -\frac{1}{2M}\frac{\left(\int V\right)_{\mp}}{\left(\int A\right)_{\mp}} \\ &= -\frac{1}{2M}\frac{\left(\int V\right)_0}{\left(\int A\right)_{\mp}}\frac{\left(\int V\right)_{\mp}}{\left(\int V\right)_0} \\ &= -\frac{1}{2M}\frac{\left(\int V\right)_0}{\left(\int A\right)_{\mp}}\frac{\left(\int \boldsymbol{\sigma}\right)_{\mp}}{\left(\int \boldsymbol{\sigma}\right)_0}, \end{aligned} \tag{17}$$

where the subscripts $-$, $+$, and 0 stand for the electron, positron, and γ decays, respectively. In Eq. (17), $(\int V)_0$ and $(\int A)_{\mp}$ can be determined experimentally. There are, however, no experimental data on $(\int V)_{\mp}$ to good enough precision for our purpose. We adopt theoretically estimated values $(\int \boldsymbol{\sigma})_{\mp}/(\int \boldsymbol{\sigma})_0$ in place of $(\int V)_{\mp}/(\int V)_0$. The approximation is justified since the nuclear matrix elements of the isovector current $\int V$ is dominated by $\mu \int \boldsymbol{\sigma}$ and a small contribution of less than 1% from $\int \boldsymbol{l}$ term, which may depend on the charge asymmetry. This means that the possible asymmetry of the weak magnetism contributes only a small fraction of the 1%. Although there is a possible contribution of 2.9% for the exchange currents to the individual matrix elements $\int \boldsymbol{\sigma}$, the effects are mostly canceled in the ratio $(\int \boldsymbol{\sigma})_{\mp}/(\int \boldsymbol{\sigma})_0$. The nuclear model we have adopted in calculating $(\int \boldsymbol{\sigma})_{\mp}/(\int \boldsymbol{\sigma})_0$ is given in the next section. The nucleon wave functions are found so as to fit the separation energy of each nucleon. For ^{12}C we adopt an average of nucleon wave functions for ^{12}B and ^{12}N. In this model we have $(\int \boldsymbol{\sigma})_{\mp}/(\int \boldsymbol{\sigma})_0 = 1.026$ and 0.975 for the electron and positron decays, respectively.

Now we derive $(\int V)_0$ and $(\int A)_{\mp}$ for the experimental data of the γ- and β-transition rates. The γ-decay width of the analog $M1$ transition ^{12}C* (15.11 MeV) $\rightarrow$ ^{12}C (ground state) is precisely measured through the photon or the electron scattering on ^{12}C. The γ-decay width Γ_γ can be written as $\Gamma_\gamma = |(\int V)_0|^2 \alpha E_\gamma^3/6M^2$, where E_γ is the energy of the γ ray under consideration and α is the fine structure constant. The Γ_γ was evaluated from the 12 data of experiments [22], which employed photon or electron scattering. The weighted mean value of all the available data is $\Gamma_\gamma = (38.2 \pm 0.6)$ eV. In the derivation of $(\int V)_0$, the isospin mixing of the $T = 0$ component from the 12.71-MeV excited state in ^{12}C was properly taken into account [23]. An admixture of 6% given in the study of the electron scattering [24] is adopted in the present analysis. The 6% isospin mixing results in an enhancement of the weak magnetism by 0.6% and thus the effect of the possible variation of the assumed value of the mixing on the weak magnetism is small. The ratio of the ft values of the Gamow-Teller transition and the super allowed $0 \rightarrow 0$ transition is related to the axial vector matrix element as in the following formula:

$$\frac{ft_{0\rightarrow 0}}{ft_{\mp}} = \frac{\left|\left(\int A\right)_{\mp}\right|^2}{2f_V^2}. \tag{18}$$

The experimental ft values adopted are $ft(^{12}\mathrm{B}) = (11\,668 \pm 54)$ s and $ft(^{12}\mathrm{N}) = (13\,183 \pm 91)$ s. We obtained the ratio of nuclear matrix elements,

$$\frac{\left(\int V\right)_-}{\left(\int A\right)_-} = -4.02 \pm 0.03 \quad \text{and} \quad \frac{\left(\int V\right)_+}{\left(\int A\right)_+} = -4.06 \pm 0.03. \tag{19}$$

Finally, the experimental value of the weak magnetism is determined to be

$$a = \frac{4.04 \pm 0.03}{2M} \tag{20}$$

in the 1σ level, where the error comes from the contribution of the statistical error of Γ_γ and ft values, which is taken into account as a systematic error in the final result. We notice here that the different nuclear models for $(\int \boldsymbol{\sigma})_{\mp}/(\int \boldsymbol{\sigma})_0$ do not introduce any significant effect to the numerical value in Eq. (20).

C. Possible asymmetry in the axial charge

Possible charge asymmetry in the mirror β decays was once discussed in connection with the ft-value ratio of the p-shell nuclei. Deviation from unity of this ratio is expected if there is a difference of nuclear structure in mirror nuclei. (There would be the effect originated from the induced tensor current in the β decay. This was eliminated in the case of the mass $A=8$ system by studying the dependence on the maximum electron energy [25].) Blomqvist explained this asymmetry by investigating the difference of the nuclear structure due to the binding energy difference of the decaying nucleons in the mass $A=12$ system [26]. At the same time, Wilkinson made an extensive investigation on the same subject with an essentially identical method as that of Blomqvist in a wide range of the $0p$-sd-shell nuclei and discussed nuclear structure effects [27]. As is seen in these two investigations, the mirror asymmetry of the Gamow-Teller matrix elements is sizable due to the charge asymmetric nuclear structure. Thus it would be worthwhile to study such an effect in the axial charge, even though most of the investigations of β-ray angular distribution or correlation-type experiments usually assume the charge symmetry for the mirror decays, because the physical observables in these experiments are related to the ratio of the nuclear matrix elements. For the present measurement of the alignment correlation term, not only are the counting statistics high but also the experimental technique and the theoretical analysis are reliable enough to consider such contribution from charge asymmetry.

The strength of the induced tensor current is derived from the observed quantity with an estimated value of Δy given by a theory, see Eq. (5). Here y is defined by the ratio of the axial charge to Gamow-Teller matrix elements, $y=-2M\int i\gamma_5 \mathbf{r}/\int \boldsymbol{\sigma}$, and Δy is the difference of $y_-(^{12}\mathrm{B})$ and $y_+(^{12}\mathrm{N})$. We have two publications available for Δy. First of all we introduce here the theoretical values of Δy in Ref. [14]. They adopted the method by Blomqvist [26] but with the Hauge-Maripuu model [28] with seven parent states for the residual $A=11$ system. (Ref. [26] adopted the Cohen-Kurath model [29] with three parent states.) The Wood-Saxon central potential depth parameter is varied so as to fit the correct separation energy for the decaying nucleon for each parent states, which is 3.370 MeV for ^{12}B and 0.601 MeV for ^{12}N. Potential parameters other than the central depth are the same as those in Ref. [26]. As a result, they obtained $\Delta y=0.10$ (denoted by the Blomqvist model in Ref. [14]) with a good fit to the ft-value ratio. In order to see a variation of the value Δy by a simplified model, they assumed a similar model as above but with a fixed Wood-Saxon central potential of 40.2 MeV by neglecting the parent state dependence. This model (denoted by WSWF in Ref. [14]) gives $\Delta y=0.13$, with a fairly large deviation of the ft-value ratio from experimental data. They also gave a value of $\Delta y=0.22$ for a simple harmonic oscillator model by adjusting the oscillator strength parameters to fit the observed ft-value ratio, just for the purpose of estimating the order of magnitude for Δy. Therefore, this value is not used in our further discussion. On the other hand, we have to refer the paper of Guichon and Samour [30], which studied possible charge asymmetry in nuclear form factors appearing in the β decays of the $A=12$ system. They estimated this asymmetry by multiplying transition operators with the factors whose numerical values are those of overlapping integrals of the single-particle wave functions in Blomqvist's work [26]. This method is, in principle, good for the Gamow-Teller matrix elements but not justified for the axial charge operator, since it contains the derivatives of nucleon coordinates through the nucleon momentum operator. In Ref. [14], this is correctly performed by taking into account the derivative operators operating on the nucleon wave functions explicitly. Although there is no explicit value of Δy in Ref. [30], we can easily evaluate it by using their numerical tables. We obtained $\Delta y=0.058$ for the Hauge-Maripuu model. Furthermore, we can also use their numerical tables for the Cohen-Kurath model and we obtain $\Delta y=0.059$. This shows that the variation due to configuration mixing parameters is negligible, at least, for Δy, although it is sizable for absolute values of matrix elements and there still remains the effect of the derivative operator.

Finally, we adopt here the theoretical value

$$\Delta y=\frac{y_+(^{12}\mathrm{N})-y_-(^{12}\mathrm{B})}{2}=0.10\pm 0.05\ \ (\text{theory}). \quad (21)$$

The ambiguity ± 0.05 is conservatively assumed to cover two other values 1.13 and 0.06. In the analysis, we evaluated our present experimental result as

$$\left(2M\frac{f_T}{f_A}\right)_{\text{expt}}=\left(2M\frac{f_T}{f_A}\right)_{\text{fit}}+\Delta y. \quad (22)$$

Here the contribution of the exchange currents to Δy is relatively small compared with the above Δy values. This is because the matrix elements of the axial charge due to the exchange currents consists of parts coming from the core and valence nucleons while those in the impulse approximation are due to the valence nucleons only.

D. Systematic corrections and errors

We made some systematic corrections to our experimentally determined alignment correlation terms and evaluated the uncertainties of the corrections and considered systematic errors. Correction factors denoted by C_i are defined as

$$\left[\frac{B_2(\hat{E}_j)}{B_0(\hat{E}_j)}\right]_{\text{Corr}}=\prod_i C_i\times\left[\frac{B_2(\hat{E}_j)}{B_0(\hat{E}_j)}\right]_{\text{Uncorr}}, \quad (23)$$

where i's are Ω, P, branching ratio (BR), response (RES), and HD defined below and j ranges from 5 to 13 MeV for ^{12}B and from 5 to 15 MeV for ^{12}N by 1-MeV steps. Since the alignment was deduced from the observed polarization averaged over β-ray energy, corrections to the observed polarization and hence to the alignment are energy independent. Corrections of the alignment correlation terms themselves are energy dependent. The correction factors considered in the present analysis are summarized in Table

TABLE II. Correction to the alignment correlation terms and systematic errors. The values of energy-independent part multiplied by the energy-dependent part $C(E)$ shown in Fig. 7 are listed, where E is the β-ray total energy. The values of the systematic errors are given in relative percentage to the alignment correlation coefficient and the absolute values of the total systematic errors are shown in the last row.

	^{12}B		^{12}N	
Correction	C	error (%)	C	error (%)
Solid angle	1.054	0.33	1.055	0.36
$\langle p/E \rangle$	0.997	<0.01	0.998	<0.01
Polarization correlation term	1.001	0.01	0.974	0.02
Alignment calculation		0.08		0.24
Energy scaling		0.50		0.50
Beam position		0.80		0.20
Catcher thickness		0.29		0.28
Decay branch [a]	$0.988C_{\mathrm{BR}}(E)$	0.03	$0.977C_{\mathrm{BR}}(E)$	0.03
Counter response [a]	$C_{\mathrm{RES}}(E)$	0.80	$C_{\mathrm{RES}}(E)$	0.81
HD^+ admixture [a]			$0.990C_{\mathrm{HD}}(E)$	0.13
Sum		1.31		1.11
Total systematic error in alignment correlation coefficient $(1/2M)$		<0.01		0.06

[a]These corrections have contributions from both the energy-independent and -dependent parts.

II. The energy-dependent corrections are illustrated in Fig. 7 in solid lines together with the total correction in dotted lines. The effects of the corrections of the alignment correlation terms on $2Mf_T/f_A$ and y can be roughly estimated from the change of the slope of the alignment correlation terms as a function of the β-ray energy (alignment correlation coefficient) as shown in Eq. (5). The systematic errors are also shown in Table II in relative percentage to the slope. Each correction is explained briefly below.

a. The finite solid angle of the β-ray detectors. The degree of alignment was deduced from the polarization. The polarization term, however, has a different angular distribution from that of the alignment. Since the counter solid angle was finite, the observed polarization is the average of the $P_1(\cos\theta)$ dependence over the present solid angle while the alignment correlation term is the average of $P_2(\cos\theta)$ dependence as shown in Eq. (3). Thus the calculated alignment correlation term has a correction factor $\int P_1(\cos\theta)d\Omega/\int P_2(\cos\theta)d\Omega$. The actual angular distribution, however, suffers from the scattering effect caused by the Mg catcher and thus the distribution is modified. This was taken into account by the EGS4 simulation [20]. The correction factor C_Ω is then given by

$$C_\Omega = \frac{\int\int P_1(\cos\theta)g(\theta,E)S(E)dEd\Omega}{\int\int P_2(\cos\theta)g(\theta,E)S(E)dEd\Omega}, \qquad (24)$$

where $g(\theta,E)$ is the scattering effect of the β rays emitted from the catcher. The correction factor affects the slope of the alignment correlation terms by $+5.38\%$ for ^{12}B and $+5.51\%$ for ^{12}N.

b. β-ray energy dependence of the angular distribution. In the β-ray angular distribution, the polarization term is given by $\mp P(p/E)(B_1/B_0)P_1(\cos\theta)$. Because the factor $(p/E)B_1/B_0$ is slightly deviated from unity, the difference needs to be corrected. The correction factor C_P is energy independent and is given by

$$C_P = \frac{\int\int S(\mu)P(p/E)(B_1/B_0)R(\mu,E)d\mu dE}{\int\int S(\mu)R(\mu,E)d\mu dE}, \qquad (25)$$

where the $R(\mu,E)$ is the counter-response function. This factor affects the slope of the alignment correlation terms by -0.21% for ^{12}B and -2.82% for ^{12}N.

c. β-decay branches. The β decays of ^{12}B and ^{12}N have small decay branches to the excited states of ^{12}C. Since the branch to the first excited state has a different maximum β-ray energy and a change of spin $1^+ \rightarrow 2^+$ from that of main branch to the ground state, which results in the change of angular distribution, the measured alignment and polarization are distorted due to the small mixture from the branch. The latest branching ratios (1.28% and 1.898% for ^{12}B and ^{12}N, respectively) were used for the correction. The energy-dependent part $C^A_{\mathrm{BR}}(E)$ and energy independent part C^P_{BR} of the correction factors are given by

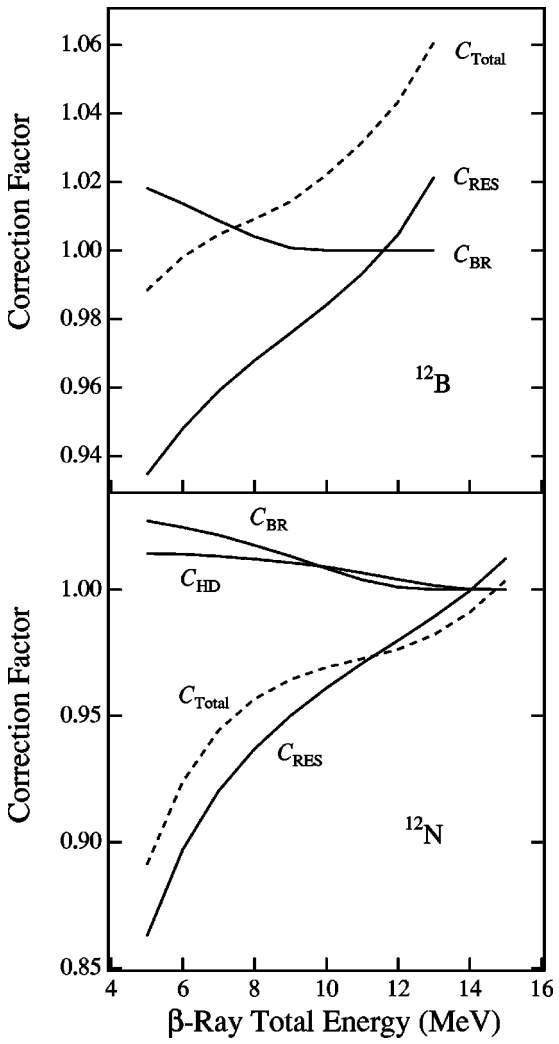

FIG. 7. Energy-dependent and total correction factors. The total correction factor is defined in Eq. (23) as $C_{\rm Total}=\Pi_i C_i$. The energy-dependent correction factors for ^{12}B(upper) and ^{12}N(lower) are shown in the solid lines as functions of β-ray total energy in the analyzed energy region. The dotted lines are the total correction factors, which include energy-independent part. Each correction factor is defined in Sec. IV D.

$$C^A_{\rm BR}(E)=\left[1-\frac{9}{10}\frac{\int S_1(\mu)R(\mu,E)d\mu}{\int S(\mu)R(\mu,E)d\mu}\right]^{-1},$$

$$C^P_{\rm BR}=1-\frac{3}{2}\frac{\int S_1(\mu)R(\mu,E)d\mu dE}{\int S(\mu)R(\mu,E)d\mu dE}, \qquad (26)$$

respectively. Here S_1 is the β-ray spectrum of the decay to the first excited state of ^{12}C. These factors affect the slope of the alignment correlation terms by -0.42% for ^{12}B and -1.48% for ^{12}N.

d. Response function of the β-ray detectors. The observed β-ray energy spectrum is distorted from its original statistical shape due to the response of the β-ray counter as discussed above. Because of the response, the alignment effect at the given energy spreads out into another energy region. The correction factor $C_{\rm RES}(E)$ for this effect is energy dependent and is given by

$$C_{\rm RES}(E)=E\frac{\int S(\mu)R(\mu,E)d\mu}{\int S(\mu)\mu R(\mu,E)d\mu}, \qquad (27)$$

which affects the slope of the alignment correlation term by -3.86% for ^{12}B and -4.07% for ^{12}N.

e. Admixture of the HD^+ *beam in the* ^{3}He *beam*. In the production of ^{12}N a small but finite admixture of HD^+ beam produced ^{12}B, to disturb the measured ^{12}N energy spectrum. The HD^+ can be mixed in the ^{3}He beam through the residual H and D atoms on the wall of the ion source and in the canal of the gas inlet forming HD molecules, and ionized and accelerated by the Van de Graaff accelerator. Since the mixed HD^+ in ^{3}He beam cannot be separated out by the analyzer magnet, it hit residual ^{11}B in the ^{10}B enriched target [^{10}B(90.4%; ^{11}B 9.6%) or ^{10}B (99.8%; ^{11}B 0.2%)] and produced unwanted ^{12}B through the ^{11}B$(d,p)^{12}$B reaction. Due to large cross section of the (d,p) reaction, this contamination can be significant with even a small admixture. This contamination was monitored from the analysis of the β-ray time spectra and the polarization correlation term, which is sensitive to the admixture of ^{12}B, to obtain the ratio of the yield of the unwanted ^{12}B to that of ^{12}N to be $(1\pm0.5)\%$. The energy-dependent part $C^A_{\rm HD}(E)$ and energy-independent part $C^P_{\rm HD}$ of the correction factors are given by

$$C^A_{\rm HD}(E)=\frac{\int [S(\mu)+S_{\rm mix}(\mu)]d\mu}{\int S(\mu)R(\mu,E)d\mu},$$

$$C^P_{\rm HD}=\frac{\int\int S(\mu)R(\mu,E)d\mu dE}{\int\int [S(\mu)+S_{\rm mix}(\mu)]R(\mu,E)d\mu dE}, \qquad (28)$$

respectively. Here, $S_{\rm mix}$ is the mixed ^{12}B energy spectrum. These factors affect the slope of the alignment correlation terms by -0.25% for ^{12}N.

f. Propagation of the error in the observed alignment. The error in alignment affects evenly all the data points of different energy bins. Although the origin of the effect was statistical, the error was taken into account as a systematic error from the nature of the error.

g. Energy scaling. The energy scale was experimentally determined by producing several β-emitting unstable nuclei and by detecting their end-point energies. The nonlinearity of the scale, which was mainly caused by the gain shift of the counter system during the long run, directly affects the slope of the alignment correlation term but the sensitivity of the present procedure to the nonlinearity is limited. The stability

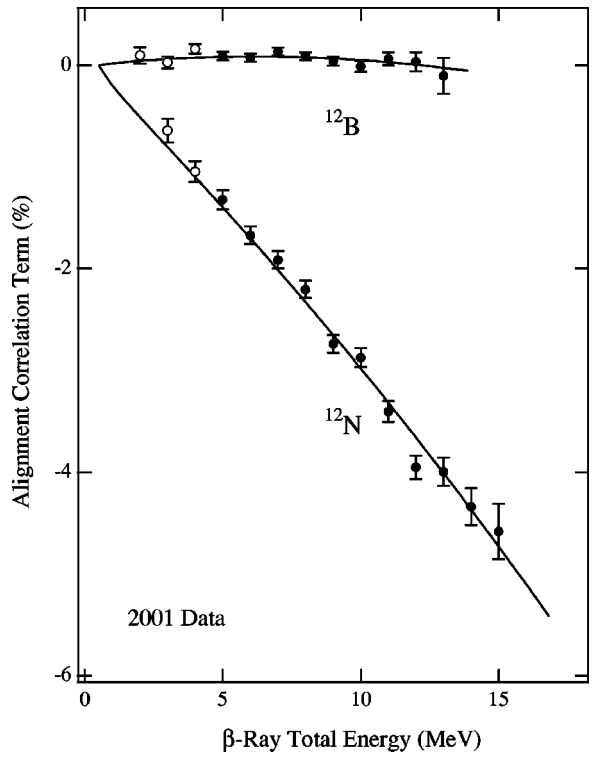

FIG. 8. Alignment correlation terms of ^{12}B and ^{12}N obtained in the present study. The corrected alignment correlation terms of ^{12}B and ^{12}N are shown as functions of β-ray total energy. The full circles are the data used in the extraction of the final result and open circles are not. The solid lines are the theoretical curve's best fit to the present data. $\chi^2/\nu=1.02$ was obtained.

of the counter system was monitored by the change in the center of gravity of the β-ray energy spectrum and was found to be within $\pm 1\%$ for both the ^{12}B and ^{12}N experiments. The possible effect within the present sensitivity was taken into account as a systematic error.

h. Incident beam position on the target. The gravitation center of the incident beam irradiated on the production target may slightly move within the designed region during the long run, which resulted in a slight change in the distribution of the recoiling nucleus on the surface of the catcher. The β-ray scattering effect and the energy loss in the catcher depends on that distribution and thus is affected by the beam position changes. This effect was evaluated by the EGS4 simulation and taken into account as a systematic error.

i. Catcher thickness. As previously described, the Mg catcher was etched every 72 h because of the decrease in the polarization due to the contamination on the surface of the catcher. Each time the Mg catcher was etched, its decrease in thickness affected the β-ray scattering effect and the energy loss in the catcher. The effect was evaluated by the EGS4 simulation and taken into account as a systematic error.

V. RESULT AND DISCUSSION

The alignment correlation terms were obtained as a function of the β-ray total energy as shown in Fig. 8 after the careful consideration of the corrections and errors. In this figure the full circles are the present alignment correlation terms used in the extraction of the final result and the open circles at low β-ray energy are not. The solid line is the theoretical curve's best fit to the data as discussed below.

TABLE III. Result of the theoretical curve best fits to the data. The results of the data obtained in the present and 1996 studies are summarized. Errors are evaluated at a 90% CL and all the values are in units of $1/2M$. The asymmetry in the axial charge $\Delta y = 0.10 \pm 0.05$ discussed in Sec. IV C was used.

Study	$2Mf_T/f_A$	Error		
		stat.	syst.	theory
Without Δy				
Present	-0.31	0.09	0.07	
Previous (1996)	-0.02	0.17	0.15	
With Δy				
Present	-0.21	0.09	0.07	0.05
Previous (1996)	$+0.08$	0.17	0.15	0.05
Mean	-0.15	0.12		0.05

Study	y	Error	
		stat.	syst.
Present	4.96	0.09	0.05
Previous (1996)	4.65	0.17	0.14
Mean	4.90	0.10	

A. Results of our present study

The *G*-parity irregular induced tensor term should be determined by considering the higher-order effects. With this in mind, we have adopted a formulation of the angular distribution, which introduces higher-order partial waves for leptons, Coulomb corrections for the finite size of nuclei, and radiative corrections [15,16]. Using the full formula, we have made a least χ^2 fit of the theoretical curves for ^{12}B and ^{12}N simultaneously to a set of ^{12}B and ^{12}N data resulting in slightly curved lines for alignment terms as functions of β-ray energy shown in Fig. 8 as solid lines. The experimental data points used for the extraction of the final result were from 4.5 MeV to 13.5 MeV (data points of 5 MeV–13 MeV in Fig. 8) for ^{12}B and from 4.5 MeV to 15.5 MeV (data points of 5 MeV–15 MeV in Fig. 8) for ^{12}N. The free parameters for the fit were f_T and the axial charge y.

From the fit of the theoretical curves to the experimental data, we obtain the results listed in Table III, where we had the reduced χ^2 minimum, $\chi^2/\nu=1.02$, ν being the degree of freedom of the fit. In order to extract f_T, the experimentally determined weak magnetism, $a=(4.04\pm 0.03)/2M$, given in Sec. IV B was used. We have $2Mf_T/f_A=-0.31\pm 0.09$ (stat.) ± 0.07 (syst.) and $y=4.96\pm 0.09$ (stat.) ± 0.05 (syst.) at a 90% confidence level (CL), where the possible asymmetry in the axial charges is not initially taken into account. Finally, considering the charge asymmetry in the axial charge, $\Delta y=0.10\pm 0.05$, discussed in Sec. IV C, we obtained the

form factor of the *G*-parity irregular induced tensor term from the data obtained in the present study as

$$2M\frac{f_T}{f_A} = -0.21 \pm 0.09 \ \text{(stat.)} \pm 0.07 \ \text{(syst.)} \pm 0.05 \ \text{(theory)} \tag{29}$$

at a 90% CL. This result is consistent with but more precise than previous results [12,13]. The induced tensor term is vanishingly small and *G* symmetry is well maintained.

B. Combined results of our present and earlier studies

To combine the present result with the previous one obtained in the year 1996 [13], we applied newly studied systematic corrections to the alignment correlation terms obtained in the work of [13] and considered systematic errors. We did not include results obtained in 1985 and 1992, which were also discussed in [13] because they have large systematic errors resulting from the counter response and from the unknown hyperfine interaction in the Mg catcher at that time, which has been solved in the present and the Ref. [13] experiment. The main part of the reanalysis of the systematic correction was made in the β-ray scattering effect in the Mg catcher, which affects the correction of the counter solid angle. The correction factor $C_\Omega = 1.031$ for the alignment correlation terms was replaced by 1.054 for ^{12}B and by 1.055 for ^{12}N. As a result from the reanalyzed data obtained in the year 1996 we have

$$2M\frac{f_T}{f_A} = +0.08 \pm 0.17 \ \text{(stat.)} \pm 0.15 \ \text{(syst.)} \pm 0.05 \ \text{(theory)} \tag{30}$$

at a 90% CL. The systematic errors due to the β-ray scattering was added, which turned out to be small relative to the original one. In this result the asymmetry in the axial charge was taken into account. Finally, combining the previous and present results we have

$$2M\frac{f_T}{f_A} = -0.15 \pm 0.12 \pm 0.05 \ \text{(theory)} \tag{31}$$

at a 90% CL. Here the quadratic sum of the statistical and the systematic errors was used for the weight of the sum. In another form, adding these errors we have

$$-0.31 \leqslant 2M\frac{f_T}{f_A} \leqslant 0.02 \tag{32}$$

at a 90% CL. The induced tensor term turns out to be vanishingly small and *G* symmetry is maintained. Recently, a theoretical prediction of f_T [11] was calculated based on the QCD sum rules. In this QCD framework f_T is proportional to the mass difference between the up and down quarks roughly estimated to be $2Mf_T/f_A \sim (m_u - m_d) \sim 0.004$. The precise calculation gives $2Mf_T/f_A = +0.0152 \pm 0.0053$, which is consistent with the present experimental limit. Here the free quark masses, $m_u = 5$ MeV and $m_d = 9$ MeV, were used. It is noted that the contribution from the electromagnetic effect is small.

C. Kubodera-Delorme-Rho model

Since our focus is with β decay of complex nuclei, in the formalism, any *G*-parity irregular signal will stem from the $NNe\nu$ vertex and meson exchange current effects. In the following we take into account the mesonic contribution and the off-shell effect following the Kubodera-Delorme-Rho (KDR) model [31]. In the formalism we consider the process $\omega \to \pi e \nu$ to be the most likely direct mesonic source of a *G*-parity violating current, since the $\omega N\bar{N}$ coupling constant is large and the ω is the lightest meson with appropriate quantum numbers. The ω meson is emitted by one nucleon and the π is absorbed by another, the $\omega \to \pi e \nu$ decay taking place between the two nucleons. The $\omega \to \pi e \nu$ process is *G*-parity irregular because ω and π are of the same *G* parity while the *G* parity associated with the leading term changes sign in the axial weak hadronic current. In a complex nuclei, nucleons are of the off-shell. The induced tensor term takes the expanded form

$$if_T \sigma_{\lambda\rho} k_\rho \gamma_5 \to i(f_T \sigma_{\lambda\rho} k_\rho \gamma_5 + if_T' P_\lambda \gamma_5). \tag{33}$$

Here the second term is associated with an exchange-π induced $N\bar{N}$ pair and k and P refer to the difference and the sum of the initial and final nucleon four-momenta, respectively. This leads us to define the constant

$$\zeta = -(f_T + f_T'). \tag{34}$$

The $\omega \to \pi e \nu$ exchange term is measured by a form factor F_ω, which leads to the exchange related constant

$$\lambda = \frac{m_\pi^3 g_{\pi NN}^2}{24\pi M^2}\left(f_T' - \frac{g_{\pi NN} F_\omega}{g_{\pi NN} m_\omega^2}\right). \tag{35}$$

In this model the correlation coefficient is denoted by κ and is expressed by using a parameter containing the coupling constants for exchange and off-mass-shell currents λ as

$$\kappa = \zeta + \lambda L \approx -f_T, \tag{36}$$

where L is the matrix element of the two-body-transition operators [31,32]. In the KDR model, thus, the *G*-parity irregular observables may be expressed with a combination of ζ and λ and these contributions cannot be separated in a single experiment on a single pair of mirror transitions.

To set a constraint on the KDR parameters with the results of the latest correlation experiments in other mass systems, we will follow the analysis in Ref. [32]. For this purpose, the statistical error of the present result in Eq. (31), which was evaluated at a 90% CL, is reduced to the 1σ level to have $2Mf_T/f_A = -0.15 \pm 0.09 \pm 0.05$ (theory) in order to combine the other experimental results. From the present result we have $\kappa = -(0.10 \pm 0.09) \times 10^{-3}$ MeV^{-1}. Also we have $\kappa = -(0.19 \pm 0.18) \times 10^{-3}$ MeV^{-1} from the β-α correlation experiment in the mass $A = 8$ [8,33], and $\kappa = -(0.27$

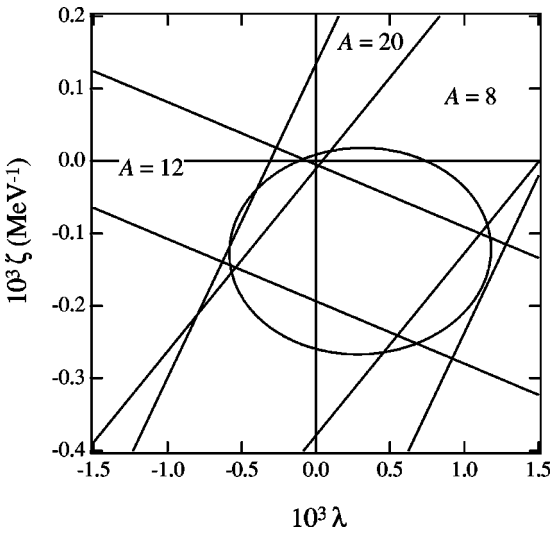

FIG. 9. Limits on the KDR parameters. The slopes indicated by the mass $A=8$ and 20 are the experimental results from [8,33] and [9,34], respectively. The ellipse is the $\chi^2=1$ contour.

$\pm 0.40)\times 10^{-3}$ MeV^{-1} from the β-γ correlation experiment in the mass $A=20$ [9,34]. The constraint on the KDR parameters is shown in Fig. 9. In this extraction we used the values of L without short range correlation in Ref. [32]. The solid ellipse is a $\chi^2=1$ contour for these three correlation experiments. We derive in the 1σ level,

$$\zeta = -(0.12\pm 0.14)\times 10^{-3}\ \text{MeV}^{-1},$$

$$\lambda = +(0.30\pm 0.88)\times 10^{-3}. \qquad (37)$$

Here it has to be noted that the present result was corrected for nuclear-structure-dependent binding energy effects Δy and the other two were not. For a more detailed discussion, we are going to measure the alignment correlation terms in the mass $A=8$ and 20 systems. Also theoretical studies in binding energy difference between mirror pairs and in the matrix element of the two-body-transition operators L are highly needed.

VI. CONCLUSION

We have measured the alignment correlation terms in the β-ray angular distributions from ^{12}B and ^{12}N. In order to eliminate the largest systematic error in the previous experiment a new timing program for spin manipulation and β-ray counting was developed. This resulted in reducing the systematic error by 1/2. Also the β-ray energy counter response to the monochromatic β ray was studied by means of the Monte Carlo simulation code EGS4. As a result a good agreement between the experimental β-ray energy spectrum and the simulated one was accomplished. From the present measurement we have the coefficient of the induced tensor term as $2Mf_T/f_A=-0.21\pm 0.09$ (stat.) ± 0.07 (syst.) ± 0.05 (theory) at a 90% CL, which is consistent with but more reliable than previous results. If we combine the present result with the previous result in 1996 [13], the corrections and systematic errors of which were newly considered and applied, we have $2Mf_T/f_A=-0.15\pm 0.12\pm 0.05$ (theory) at a 90% CL, which is consistent with the theoretical calculation based on QCD in which the induced tensor coefficient is proportional to the mass difference between up and down quarks. In the framework of the KDR model we determine the amplitude of the G-parity violating parameters ζ that originate from the $NNe\nu$ term and the exchange and off-mass-shell currents λ, as $\zeta=-(0.12\pm 0.14)\times 10^{-3}$ MeV^{-1} and $\lambda=+(0.30\pm 0.88)\times 10^{-3}$ in the 1σ level. In this extraction the results of correlation type experiments in the mass $A=8$ and 20 other than our result were considered. Here the binding energy difference between mirror pairs has been considered only in the mass $A=12$ system. In order to have a more accurate result, the measurement of the alignment term in the mass $A=8$, 20 and other mirror mass systems are going to be performed. Also the theoretical works on the charge asymmetry between mirror pairs and on the nuclear-model-dependent matrix L are very much awaited.

ACKNOWLEDGMENTS

The authors express their thanks to G. F. Krebs at Lawrence Berkeley National Laboratory for valuable discussions. We also would like to thank the crew of the Van de Graaff Laboratory of Osaka University, M. Sakamoto, T. Sakurai, and K. Ohsawa. The present work was financially supported in part by the Japan Society for the Promotion of Science for Young Scientists and by the Grant-in-Aid for Scientific Research from the Ministry of Education, Culture and Science, Japan, and also by the Yamada Science Foundation.

[1] T. Hatsuda, H. Hogaasen, and M. Prakash, Phys. Rev. C **42**, 2212 (1990).
[2] S. Weinberg, Phys. Rev. **112**, 1375 (1958).
[3] D. H. Wilkinson, Eur. Phys. J. A **7**, 307 (2000).
[4] L. Grenacs, Annu. Rev. Nucl. Part. Sci. **35**, 455 (1985).
[5] D. H. Wilkinson, Phys. Lett. **31B**, 447 (1970); D. H. Wilkinson and D. E. Alburger, Phys. Rev. Lett. **26**, 1127 (1971).
[6] K. Sugimoto, I. Tanihata, and J. Goring, Phys. Rev. Lett. **34**, 1533 (1975); F. P. Calaprice, S. J. Freedman, W. C. Mead, and H. C. Vantine, *ibid.* **35**, 1566 (1975).
[7] K. Sugimoto, T. Minamisono, Y. Nojiri, and Y. Masuda, J. Phys. Soc. Jpn. Suppl. **44**, 801 (1978); Y. Masuda, T. Minamisono, Y. Nojiri, and K. Sugimoto, Phys. Rev. Lett. **43**, 1083 (1979); H. Brandle, L. Grenacs, J. Lang, L. Ph. Roesch, V. L. Telegdi, P. Truttmann, A. Weiss, and A. Zehnder, *ibid.* **40**, 306 (1978).
[8] R. E. Tribble and G. T. Garvey, Phys. Rev. C **12**, 967 (1975); R. D. McKeown, G. T. Garvey, and C. A. Gagliardi, *ibid.* **22**, 738 (1980).
[9] N. Dupuis-Rolin, J. P. Deutsch, D. Favart, and R. Prieels, Phys.

Lett. **79B**, 359 (1978); R. E. Tribble and D. P. May, Phys. Rev. C **18**, 2704 (1978).
[10] A. Halplin, B. W. Lee, and P. Sorba, Phys. Rev. D **14**, 2343 (1976).
[11] H. Shiomi, Nucl. Phys. **A603**, 281 (1996).
[12] T. Minamisono, K. Matsuta, Y. Nojiri, and K. Takeyama, J. Phys. Soc. Jpn. Suppl. **55**, 382 (1986); T. Minamisono, A. Kitagawa, K. Matsuta, and Y. Nojiri, Hyperfine Interact. **78**, 77 (1993).
[13] T. Minamisono, K. Matsuta, T. Yamaguchi, K. Minamisono, T. Ikeda, Y. Muramoto, M. Fukuda, Y. Nojiri, A. Kitagawa, K. Koshigiri, and M. Morita, Phys. Rev. Lett. **80**, 4132 (1998).
[14] K. Koshigiri, R. Morita, and M. Morita, Nucl. Phys. **A588**, 165c (1995).
[15] M. Morita, M. Nishimura, A. Shimizu, H. Ohtsubo, and K. Kubodera, Suppl. Prog. Theor. Phys. **60**, 1 (1976); M. Morita, *Beta Decay and Muon Capture* (Benjamin, New York, 1973).
[16] M. Morita, M. Nishimura, and H. Ohtsubo, Phys. Lett. **73B**, 17 (1977); K. Koshigiri, H. Ohtsubo, and M. Morita, Prog. Theor. Phys. **66**, 358 (1981); M. Morita, R. Morita, and K. Koshigiri, Nucl. Phys. **A577**, 387c (1994).
[17] M. Morita, in *Non Nucleonic Degrees of Freedom Detected in Nucleus*, edited by T. Minamisono, Y. Nojiri, T. Sato, and K. Matsuta (Word Scientific, Singapore, 1996), p. 125.
[18] T. Minamisono, K. Matsuta, T. Yamaguchi, K. Minamisono, M. Fukuda, A. Kitagawa, and K. Koshigiri, Phys. Rev. Lett. **82**, 1644 (1999).
[19] A. Kitagawa, K. Matsuta, Y. Nojiri, and T. Minamisono, Hyperfine Interact. **60**, 869 (1990).
[20] W. R. Nelson, H. Hirayama, and D. W. O. Rogers, Stanford University, SLAC-265.
[21] C. S. Wu, Y. K. Lee, and L. W. Mo, Phys. Rev. Lett. **39**, 72 (1977); W. Kaina, V. Soergel, H. Thies, and W. Trost, Phys. Lett. **70B**, 411 (1977); J. B. Camp, Phys. Rev. C **41**, 1719 (1990); M. Fukuda, K. Mashitani, M. Mihara, A. Harada, H. Shiohara, K. Matsuta, Y. Nojiri, and T. Minamisono, in *Non Nucleonic Degrees of Freedom Detected in Nucleus*, edited by T. Minamisono, Y. Nojiri, T. Sato, and K. Matsuta (World Scientific, Singapore, 1996), p. 136.
[22] F. Ajzenberg-Selove and T. Lauritsen, Nucl. Phys. **A114**, 1 (1968); **114**, 69 (1968); B. T. Chertok, C. Sheffield, J. W. Jightbody, Jr., S. Penner, and D. Blum, Phys. Rev. C **8**, 23 (1973); U. Deutschmann, G. Lahm, and R. Neuhausen, Nucl. Phys. **A411**, 337 (1983).
[23] K. Koshigiri, M. Nishimura, H. Ohtsubo, and M. Morita, Nucl. Phys. **A319**, 301 (1979); K. Koshigiri, H. Ohtsubo, and M. Morita, J. Phys. Soc. Jpn. Suppl. **55**, 1014 (1986).
[24] J. B. Flanz, R. S. Hicks, R. A. Lindgren, G. A. Peterson, J. Dubach, and W. C. Haxton, Phys. Rev. Lett. **43**, 1922 (1979).
[25] D. H. Wilkinson and D. E. Alburger, Phys. Rev. Lett. **26**, 1127 (1971).
[26] J. Blomqvist, Phys. Lett. **35B**, 375 (1971).
[27] D. H. Wilkinson, Phys. Rev. Lett. **27**, 1018 (1971).
[28] P. S. Hauge and S. Maripuu, Phys. Rev. C **8**, 1609 (1973).
[29] S. Cohen and D. Kurath, Nucl. Phys. **75**, 1 (1965).
[30] P. A. M. Guichon and C. Samour, Nucl. Phys. **A382**, 461 (1982).
[31] K. Kubodera, J. Delorme, and M. Rho, Nucl. Phys. **B66**, 253 (1973).
[32] K. Kubodera, J. Delorme, and M. Rho, Phys. Rev. Lett. **38**, 321 (1977); M. Oka and K. Kubodera, Phys. Lett. **90B**, 45 (1980).
[33] L. De Braeckeleer, E. G. Adelberger, J. H. Gundlach, M. Kaplan, D. Markoff, A. M. Nathan, W. Schieff, K. A. Snover, D. W. Storm, K. B. Swartz, D. Wright, and B. A. Brown, Phys. Rev. C **51**, 2778 (1995), and references therein.
[34] R. D. Rosa, W. W. Daehnick, Swapan K. Saha, and P. C. Li, Phys. Rev. C **37**, 2722 (1988), and references therein.